



HAL
open science

Solvent free sol-gel based synthesis of soft magnesium silicate

Busra Findik, Valentin Cinquin, Franck Gyppaz, Christian Carrot, Véronique Bounor-Legaré

► **To cite this version:**

Busra Findik, Valentin Cinquin, Franck Gyppaz, Christian Carrot, Véronique Bounor-Legaré. Solvent free sol-gel based synthesis of soft magnesium silicate. *Journal of Sol-Gel Science and Technology*, 2022, 103 (3), pp.921-934. 10.1007/s10971-022-05852-7 . hal-03765075

HAL Id: hal-03765075

<https://hal.science/hal-03765075v1>

Submitted on 30 Aug 2022

HAL is a multi-disciplinary open access archive for the deposit and dissemination of scientific research documents, whether they are published or not. The documents may come from teaching and research institutions in France or abroad, or from public or private research centers.

L'archive ouverte pluridisciplinaire **HAL**, est destinée au dépôt et à la diffusion de documents scientifiques de niveau recherche, publiés ou non, émanant des établissements d'enseignement et de recherche français ou étrangers, des laboratoires publics ou privés.

Solvent Free Sol-Gel Based Synthesis of Soft Magnesium Silicate

Busra Findik^{1,3}, Valentin Cinquin¹, Franck Gyppaz³, Christian Carrot², Véronique Bounor-Legaré^{1*}

(1) Université Lyon, CNRS, Université Claude Bernard Lyon 1, INSA Lyon, Université Jean Monnet, UMR 5223, Ingénierie des Matériaux Polymères, F-69622 VILLEURBANNE Cédex, France

(2) Université de Lyon, CNRS, Université Claude Bernard Lyon 1, INSA Lyon, Université Jean Monnet, UMR 5223, Ingénierie des Matériaux Polymères, F-42023 SAINT-ETIENNE Cédex 2, France

(3) Nexans Research Center, Nexans France, F-69007 LYON, France

Abstract

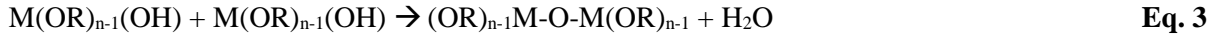
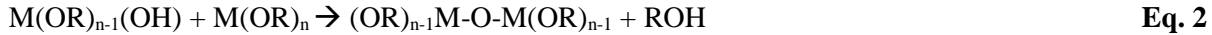
In this study, soft magnesium silicates were prepared via sol-gel method starting from diethylphosphatoethyltriethoxysilane (SiP), magnesium ethoxide and magnesium acetate. The thermal reaction of the different systems without any solvent was studied by a thermogravimetric analysis coupled to gas chromatography and mass spectroscopy in order to identify the volatile by-products and then suggest a reaction mechanism. The identification of several by-products formed during the reactions evidenced a non-hydrolytic sol-gel based route between the ethoxy and acetoxy groups of magnesium ethoxide and magnesium acetate respectively with the ethoxy groups of SiP. In addition, X-ray photoelectron spectroscopy analyses highlighted the creation of Mg-O-Si bonds. The viscoelastic behavior of the reactive systems allowed to confirm the formation of the network but also the determination of the gelation time. It corresponded respectively to 2150 and 1020 seconds for the reaction between magnesium ethoxide and SiP and magnesium acetate and SiP carried out at 170 °C. All these data confirm the formation of a “soft” inorganic networks in that range of temperature.

Keywords: magnesium silicate, solvent free, sol-gel chemistry, gel point, viscoelasticity

* Corresponding author. E-mail address: veronique.bounor-legare@univ-lyon1.fr

I. Introduction

Commonly used nowadays, the sol-gel process is a method for synthesizing a large number of inorganic compounds for many applications [1-4]. The method consisted on the formation of an oxide-based network from organometallic or silica precursors. Basically, the conversion of monomers into a colloidal solution of particles, named “sol”, followed by the formation of a continuous network enclosing the liquid phase, named “gel” occurs through condensation reactions [5, 6]. Two types of sol-gel processes have been reported: hydrolytic (HSG) and non-hydrolytic (NHSG). In the case of hydrolytic sol-gel chemistry, reactions are initiated by water which induces the hydrolysis of the inorganic precursor [7-9] (Eq.1, where R stands for an alkyl group and n the coordination number of the alkyl group around a metal or silicon atom M). Two condensation mechanisms can then be considered: alkoxolation and oxolation. The alkoxolation (Eq.2) is a reaction where an alcohol molecule is released, and the oxolation (Eq.3) a reaction where water is released. In both cases, oxo bonds M-O-M are created between metal or silicon atoms M.



In contrast to the HSG, the NHSG is based on thermoactivated reactions which uses organic oxygen donors like ether, alcohol, or alkoxide, instead of water [10]. Many mechanisms have been developed for the synthesis of oxides and they can be classified according to the oxygen donor or the nature of the released by-products during the reaction [11, 12]. Depending on the released by-product (ether, ester, or alkyl halide for example), information about the reaction mechanism can be collected and help understanding the mechanism. Eq.4 gives a reaction where ether is released during the NHSG reaction between two molecules of metal alkoxides:



In the past decades, a notable interest has been taken around the generation of mixed oxides via the sol-gel route [13-17]. Silicon alkoxides are by far the most widely used inorganic precursors in the literature. When combining with other metal precursors, these alkoxides can lead to the synthesis of mixed oxides. Lopez *et al.* [18] reported that Zr-Si mixed oxides can be synthesized by hydrolytic sol-gel technique using tetraethoxysilane (TEOS) and zirconium acetate as precursors. The authors showed that modifying the pH of the reaction medium could lead to a variation of the surface area of the created inorganic network. Other metal precursors like Ti-based ones have been used for example by Voigt [19]. Aminosilanetriols $RN(SiMe_3)(Si(OH)_3)$ with $R = 2,6-Me_2C_6H_3$, $2,6-i-Pr_2C_6H_3$ or $2,4,6-Me_3C_6H_2$ have been used with titanium orthoesters $Ti(OR')_4$ with $R' = Et$ or $i-Pr$. The reactions were carried out at room temperature for few hours in hexane. The X-ray characterization of obtained products highlighted the three-dimensional cubic cage structure and the FTIR analyses evidenced the creation of Si-O-Ti oxo bonds. Otherwise, titanium ethoxide was also used with 3-(trimethoxysilyl)propyl methacrylate and diphenylsilanediol to create UV curable silica-titania based resin through non-hydrolytic sol-gel chemistry [20]. In this case, barium hydroxide monohydrate was used as catalyst. FTIR and XPS analyses on the final product reveal the creation of Si-O-Ti bonds indicating a successful completion of the reaction between precursors after 4 hours at 80 °C.

Aluminum based precursors have also been studied in the literature in combination with different alkoxy silane. For example, aluminum nitrate was used to form boehmite sol (AlOOH) which then reacted with TEOS to synthesize aluminosilicate via hydrolytic sol-gel method [21]. The reaction was performed at a pH of 8 and at ambient temperature for 5 h. However, authors showed by ^{27}Al solid state NMR that a calcination at $400\text{ }^\circ\text{C}$ is necessary to form $\text{O}_3\text{Al-O-SiO}_3$ bonds. In a more recent paper, Bounor-Legaré and Cassagnau [22] synthesized materials containing Si-O-Al bonds. For that, aluminum acetylacetonate and tetrapropoxysilane have been used as inorganic precursors and the reaction was performed in a PP-g-MA matrix via reactive extrusion. Thanks to solid-state ^{27}Al and ^{29}Si NMR and TEM coupled with X-ray microanalyses, the authors confirmed the presence of Si-O-Al bonds.

Furthermore, magnesium based inorganic precursors have been used to create compounds containing Si-O-Mg bonds. Ciesielczyk *et al.* [23] used magnesium ethoxide and TEOS as inorganic precursor of magnesium and silicon, respectively. Ammonia solution was used to catalyze the gelation and control the condensation rate. The reaction was carried out in methanol at ambient temperature for 45 min. The obtained products were dried at $45\text{ }^\circ\text{C}$ for 24 h and then calcined at $1000\text{ }^\circ\text{C}$ for 2 h. Authors performed FTIR analyses on samples before and after calcination. They showed that Si-O-Mg bonds were formed after calcination at very high temperature. In another paper [16], silica-magnesia mixed oxides were prepared using the hydrolytic sol-gel process from magnesium chloride and TEOS with ammonia solution as catalyst. The reaction was carried out during 24 h and the final product was dried at $150\text{ }^\circ\text{C}$ for 6 h. XPS analyses confirmed the formation of Si-O-Mg bonds but also Mg-O-Mg ones. These latter bonds were attributed to the condensation of the magnesium precursor itself to form pure magnesia. Recently, magnesium acetate and TEOS have been used to synthesize MgO-SiO_2 network via hydrolytic sol-gel method [24]. The authors chose ammonia solution as catalyst and a mixture of water and ethanol as solvent. The final mixture was dried and calcined during 5 h at $500\text{ }^\circ\text{C}$. Formation of the Si-O-Mg bond was then confirmed by UV-visible and FTIR methods. Furthermore, Garnier *et al.* [25] prepared organic-inorganic talc-like hybrids using hydrolytic sol-gel chemistry. For this, magnesium nitrate and diethylphosphatoethyltriethoxysilane (SiP) were used as magnesium and silicon sources respectively. The reaction was carried out in ethanol. The effect of adding NaOH on the formation of the talc-like hybrids and related Si-O-Mg bonds was studied. After 7 h 30 min at room temperature, liquid-state and solid-state NMR evidenced the formation of Si-O-Mg bonds with or without addition of NaOH. Furthermore, it has been shown that when pH value was higher than 9, Si-O-Si bonds were cleaved, limiting the growth of the inorganic structure.

In the present work, the approach consists in studying the thermoactivated reactions between respectively a magnesium and silicon inorganic precursors and evaluating the best conditions to create a Mg-O-Si inorganic network. In that frame, two different Mg precursors, namely magnesium ethoxide and magnesium acetate tetrahydrate were used. Diethylphosphatoethyltriethoxysilane was selected as a source of Si. Sol-gel reactions were performed without using any solvent and catalyst between 120 and $170\text{ }^\circ\text{C}$. The reaction mechanism was elucidated thanks to a TGA-GC-MS coupling and XPS analyses and the kinetics were also evaluated by rheological means.

II. Experimental section

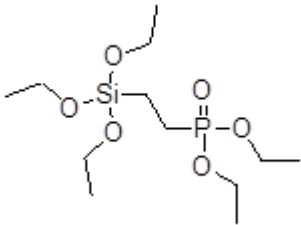
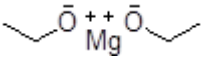
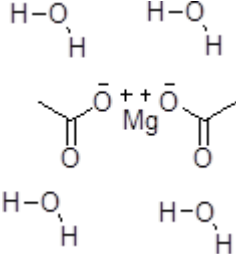
1) Materials

Magnesium sources were magnesium ethoxide (MgOEt, 98%, Acros Organics) and magnesium acetate tetrahydrate (MgAc, 98%, Alfa Aesar); both were grinded before use. Grinding was carried out in a Fritsch Pulverisette 6 planetary mill at 500 rpm for 3 min and then sieved through a 0.125 mm mesh by using a Fritsch Analysette 3 Pro vibratory sieve shaker.

The silicon source was the diethylphosphatoethyltriethoxysilane (SiP, 92%, Abcr) and was used as received without purification.

Chemical structures and main features of reagents are given in **Table 1**.

Table 1 Chemical structures of used reagents

Diethylphosphatoethyltriethoxy silane (SiP)	Magnesium ethoxide (MgOEt)	Magnesium acetate tetrahydrate (MgAc)
		
Physical state: colorless liquid	Physical state: light yellowish powder	Physical state: White powder
Molar mass: 328 g/mol	Molar mass: 114 g/mol	Molar mass: 214 g/mol
Boiling point: 340 °C @760 mmHg (from safety data sheet)	Melting point: 270 °C (from safety data sheet)	Melting point: 72-75 °C (from safety data sheet)

2) Synthesis

The reaction between SiP and MgOEt was carried out in stoichiometric conditions with equimolarity of functional ethoxysilane groups (SiP) and ethoxy groups (MgOEt). Typically, 13.73 g of magnesium ethoxide and 26.27 g of diethylphosphatoethyltriethoxysilane were added in a glass reactor vessel equipped with a paddle agitator.

The reaction with MgAc, was carried out with equimolar amounts of magnesium acetate tetrahydrate and diethylphosphatoethyltriethoxysilane. For that, 21.36 g of MgAc were added to 32.64 g of SiP in the reactor.

In this case, since water from tetrahydrate MgAc may hydrolyze ethoxysilane groups SiP, equimolarity of functional groups was not used.

3) Thermogravimetric analysis coupled to gas chromatography and mass spectroscopy (TGA-GC-MS)

Thermogravimetric analysis (TGA) coupled to gas chromatography (GC) and mass spectroscopy (MS) was used to measure the weight loss and to evidence and quantify potential by-products evolved during the reaction. Analyses were performed on a TA Instruments SDT Q600 coupled to an Agilent 6890N Network Series GC-MS. TGA was performed under helium with a flow rate of 25 ml/min starting from room temperature up to 800 °C with a ramp rate of 10 °C/min. GC column (HP-5ms) made of (5%-phenyl)-methylpolysiloxane was used and the oven was heated from 60 to 300 °C with a heating rate of 20 °C/min. MS injection and detection were done at 250 °C.

Isothermal TGA-GC-MS analyses were also performed to quantify the by-products amount. For this, TGA temperature was maintained for 30 min at 120, 150 or 170 °C with GC-MS conditions as previously reported.

4) X-ray Photoelectron Spectroscopy (XPS)

X-ray Photoelectron Spectroscopy was carried out on a PHI Quantera SXM instrument with a monochromatized Al K_α radiation at 1486.6 eV and operated at 35.7 W. For all measurements, the detection angle of photoelectrons with respect to the sample position was fixed at 45°. The wide scan spectrum was recorded at a pass energy of 280 eV. Specific regions of interest, namely, Mg (1s) and Mg (2s), Si (2p) and P (2p) regions were carried out at a pass energy of 140 eV. The depth of analyses was approximately 3 nm, and the diameter of the analyzed area was 200 μm. Each sample was analyzed two times.

5) Dynamic mechanical analysis in the sol-gel state.

The evolution of the dynamic moduli of the samples during reactions under various conditions was followed with a TA Instruments Ares G2 Rheometer in the heated chamber operated under air flow. A small quantity of reaction product was placed between two parallel stainless plates of 25 mm diameter separated by 0.8 mm gap. The rheo-kinetic study of the sol-gel reactions was performed at 120, 150 or 170 °C in oscillatory shear owing to frequency sweep and time sweep experiments with an adjustment of strain during the experiment. Before any experiments, the linear viscoelastic region of systems was determined by performing a strain sweep at 1 and 100 rad/s.

III. Results and discussion

1) Identification of the reaction mechanism

To elucidate the reaction mechanism, evolved chemical species produced directly during reaction carried out in the TGA nacelle were collected and identified by GC-MS. For this, a small quantity (approximately 40 mg) of initial inorganic precursors mixture was introduced in the TGA-GC-MS cell. To illustrate, **Fig 1.**

shows typical thermogram and associated evolution of diethyl ether peak area obtained by GC analysis obtained for the reaction of magnesium ethoxide with SiP.

First, **Fig 1a** represents the evolution of the relative weight and of its derivative with respect to temperature for a 10 °C/min temperature ramp. Two major weigh losses were observed. The first one, corresponding to nearly 24 wt%, occurred between room temperature and 230 °C. The second weigh loss corresponding to roughly 38 wt% took place from 230 °C up to 800 °C. At 800 °C, a residue of 37 wt% was obtained. Gaseous by-products produced during these two weight losses were identified by GC-MS coupling analysis. Peak areas were plotted versus temperature and were presented in **Fig 1.b**. A targeted molecule corresponding to diethyl ether was found and a proof of the reaction between the ethoxy groups of SiP and the ethoxy groups of magnesium ethoxide. Actually, for similar reactions carried out with either MgOEt and SiP alone, and analyzed by TGA-GC-MS, no diethyl ether was detected, evidencing that produced diethyl ether is exclusively brought from the reaction between MgOEt and SiP. Both peaks respectively centered at around 200 °C and 350 °C also evidenced that the diethyl ether is produced through two reactional steps and suggested a difference of ethoxy functional groups reactivity.

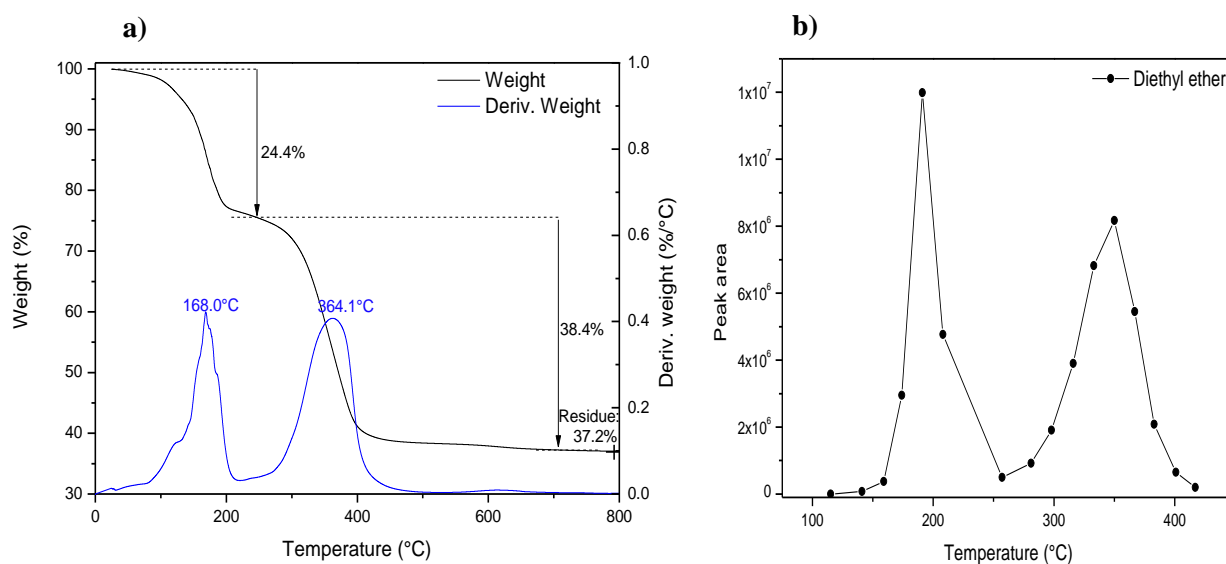


Fig. 1 (a) Thermogram obtained from the reaction carried between MgOEt + SiP in the TGA nacelle under helium and (b) corresponding evolution of diethyl ether peak area obtained by GC analysis versus temperature

From a quantitative point of view, the analysis of the amount of the residue gave some important information. Actually, theoretically, the conversion of magnesium ethoxide alone into magnesium oxide is expected at 260 °C under N₂ [26] and should produce 12 wt% of residue. When SiP is analyzed alone, a residue rate of 3 wt% is formed and attributed to an inorganic SiO₂ formation. As in the present case 37 wt% of residue was obtained (**Fig 1a**), it was assumed that 25 wt% of residue was due to the reaction with SiP. Moreover, if the reaction had been complete and if SiP was not evaporated during the coupling, the weight loss corresponding to the formation of diethyl ether would be 44 %. Experimentally, the total weight loss is about 62 % indicating that other species evaporated at the same time as diethyl ether (SiP or derivatives from POEt groups). However, in our experimental conditions, SiP was not detectable by GC-

MS. The thermogram of SiP is given in the Figure S1 of the Supplementary Information. Concerning the POEt groups, no other signal was detected in our experimental conditions able to confirm any reaction of this function.

Compared to the reaction with magnesium ethoxide, the reaction with magnesium acetate tetrahydrate was more complex and depicts three main steps as reported in **Fig 2a**. The first step took place from room temperature up to 150 °C corresponding to a weight loss of 31 wt%. The second step occurred from 150 to 230 °C with 18 wt% weight loss. Finally, from 230 to 800 °C, a third weight loss of 15 wt% was observed. At the end, at 800 °C, 36 wt% of residue was obtained. In parallel, two different volatile molecules were identified by GC-MS. During the first weight loss, ethanol is released in the range of 50 °C to 300 °C with a maximum of abundance at about 125 °C. The formation of ethanol indicates that the SiP underwent hydrolysis reaction due to the water released by the tetra-hydrated magnesium acetate. Secondly, ethyl acetate was detected at 150 °C up to almost 400 °C and presented a maximum of abundance at 200 °C. This corresponded to the second weight loss observed in TGA. Formation of ethyl acetate indicated a reaction between the ethoxysilane and/or the ethyl phosphonate groups of SiP and acetoxy groups of magnesium acetate. In theory, the conversion of magnesium acetate into magnesium oxide started around 300 °C [27, 28] and produced 7.5 wt% of residue. Therefore, it can be assumed that 28% of residue was due to the reaction between SiP and MgAc.

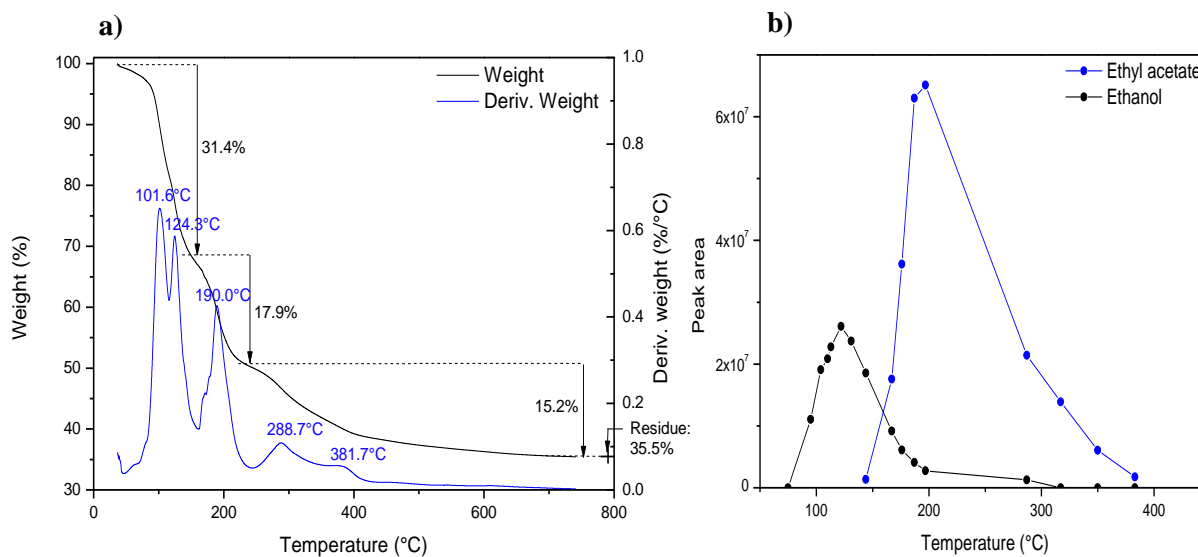


Fig. 2 (a) Thermogram obtained from the reaction carried between MgAc + SiP in the TGA nacelle under helium and (b) corresponding evolution of ethanol and ethyl acetate peak areas obtained by GC versus temperature

These results pointed out the reaction between SiP and magnesium ethoxide and magnesium acetate respectively through a thermal mechanism. These both reactions were initiated at temperature around 110 °C and 150 °C respectively in relation to the temperature at which the by-products, diethyl ether and ethyl acetate respectively, were identified. It is worth noting that with magnesium acetate, the SiP partially underwent a hydrolysis reaction.

To go further in the mechanism investigation and the potential creation of Si-O-Mg and/or P-O-Mg bonds, XPS analyses were performed on samples treated up to 260 and up to 450 °C. In **Fig 1.**, these two temperatures corresponded to the end of the first and second degradation steps. Analysis of the product after these two steps gave information about the different bonds created. Referring to the **Fig 2.**, at 260 °C almost all the ethanol was released, and an important amount of ethyl acetate was also released. 450 °C corresponded to almost the end of the weight loss.

Figure S2 in Supplementary Information presents the wide scan XPS spectrum of MgOEt + SiP and MgAc + SiP treated respectively at 260 °C and 450 °C. On these graphs, signals of different elements were observed and attributed according to the Handbook of X-ray Photoelectron Spectroscopy [29]. O (2s), O (1s) and O KLL respectively appeared at 25, 550 and 980 eV. Mg (2p), Mg (2s), Mg KLL and Mg (1s) appeared at respectively 50, 89, 307 and 1304 eV. Si (2p) and Si (2s) appeared at 102 and 151 eV, respectively. P (2p) and P (2s) appear at 133 and 190 eV, respectively and C (1s) was observed at 290 eV. All these detected elements agreed with the composition of the samples. To get further information, specific regions of interest, namely Mg (1s), and P (2p) regions were investigated.

Fig.3 shows the spectra and spectral deconvolution results of the Mg (1s) region of the reacted mixed oxides after thermal treatment at 260 °C and 450 °C respectively. For all samples, the deconvolution of the signals evidenced two components; one peak centered at 1303.3 eV assigned to Mg-O-Mg bonds [30], and another centered at 1304.7 eV attributed to Si-O-Mg bonds [16]. This latter signal is more important in intensity revealing the reaction efficiency between the magnesium and silicon derivatives through the acetoxy and ethoxy silane groups respectively. The appearance of Mg-O-Mg bonds may be related to self-condensation of magnesium precursor, independently of the reaction with SiP.

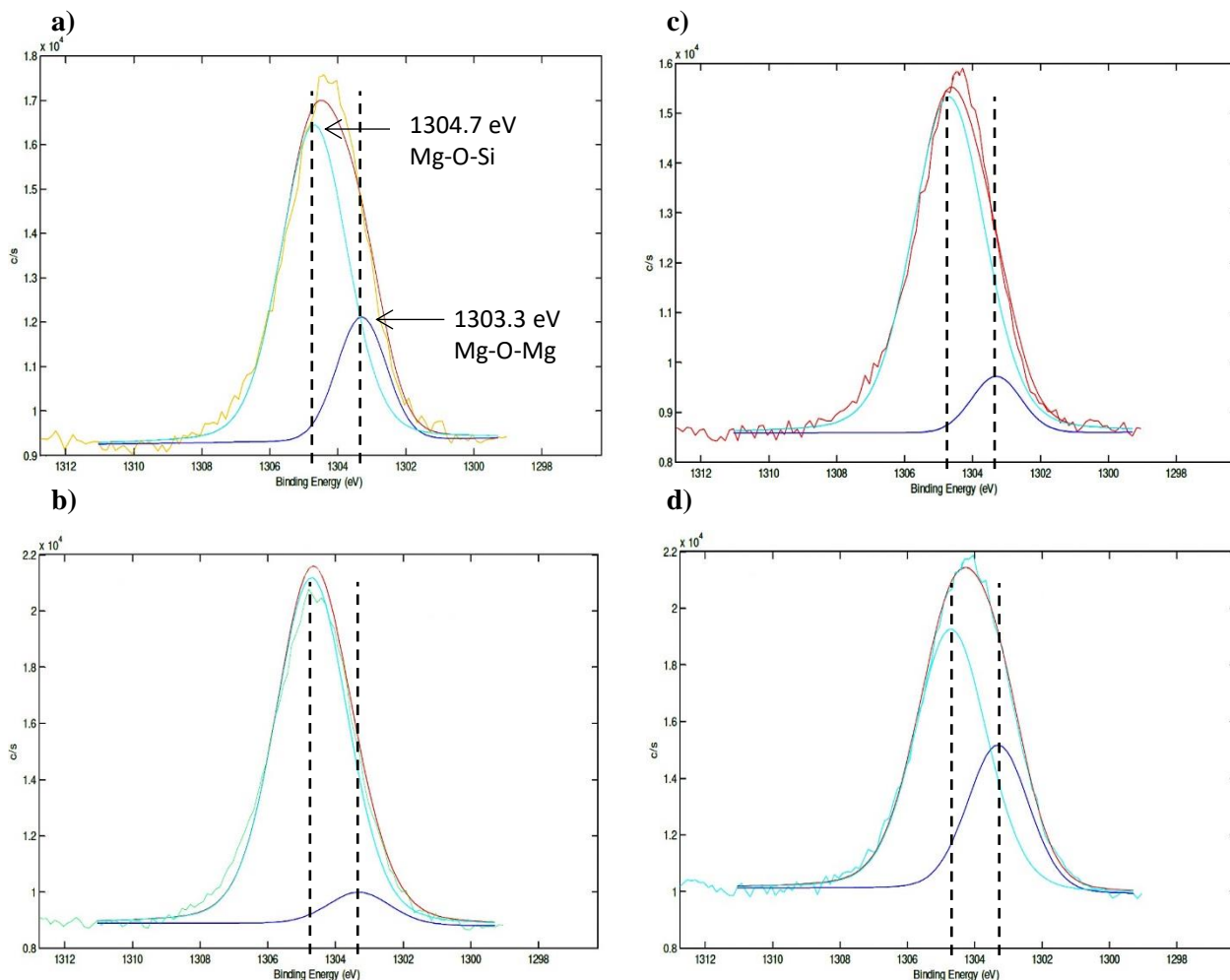


Fig. 3 Deconvolution of high resolution XPS spectra in the Mg (1s) region of MgOEt + SiP system treated at 260 °C (a); 450 °C (b); MgAc + SiP system treated at 260 °C (c) and at 450 °C (d)

Isothermal TGA-GC-MS analysis were further performed to reach a conversion rate. Thermograms are shown in the Figures S4 and S5 of Supplementary Information. Conversion rates were determined by the ratio of the number of moles of by-products produced during the weight loss observed by isothermal TGA and the theoretical number of moles of by-products expected if the reaction between both inorganic precursors was total. Results are reported in Table 2. When the temperature of the reaction increased, the conversion rate classically increased. Actually, for the system with magnesium ethoxide, the conversion rate increased from 30.4 % up to 50.5 % and up to 60.9 % after 30 min of isothermal treatment at 120, 150 and 170 °C respectively. Similarly, with magnesium acetate, the conversion rate in ethyl acetate increased from 35.3 % at 150 °C up to 66.7 % at 170 °C after 30 min of isothermal treatment. These results highlighted high conversion rates at 170 °C, i.e., over than 60 %.

Table 2 Conversion rates of MgOEt + SiP and MgAc + SiP reactions calculated from isothermal TGA-GC-MS analysis performed for 30 min

Isothermal temperature (°C)	Weight loss observed during isothermal analyses (%)	Number of moles of by-products produced during isothermal analyses (mmol)	Theoretical number of moles of by-products producible in case of total reaction (mmol)	Conversion rate (%)
MgOEt + SiP - Diethyl ether				
120	13.8	0.07	0.23	30.4
150	22.4	0.12	0.24	50.0
170	26.7	0.14	0.23	60.9
MgAc + SiP - Ethanol				
120	29.9	0.21	0.33	63.6
MgAc + SiP - Ethyl acetate				
120	<i>No peak detected</i>			
150	11.6*	0.06	0.17	35.3
170	21.0*	0.14	0.21	66.7

* The number of moles of produced by-products is calculated according to the weight loss observed during the isothermal analysis. At 150 and 170 °C, we assume that the production of ethanol is the same as 120 °C, i.e., 29.9 %.

To investigate whether any other chemical bond was created during the reaction between these inorganic precursors, P (2p) region was studied, and results (spectra and deconvolution results) are presented in **Fig 4**. A single signal was observed in the P (2p) region at a binding energy of 133.5 eV for all samples. It was assigned to the phosphonate group of SiP [31]. This indicated that the phosphonate groups of SiP were not

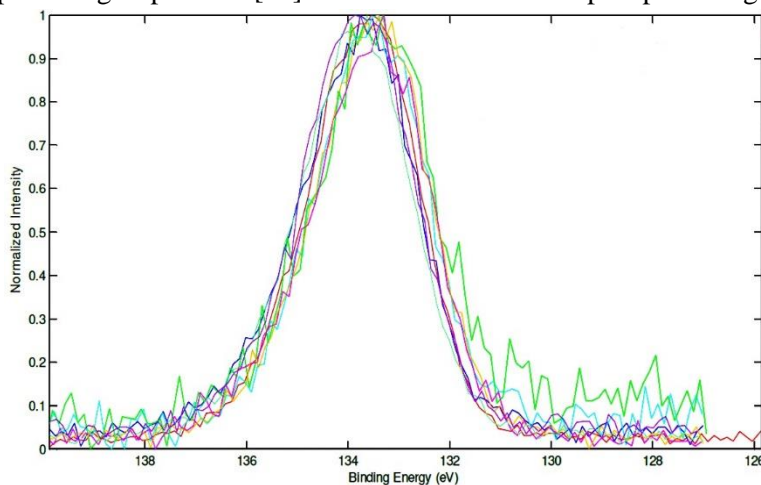


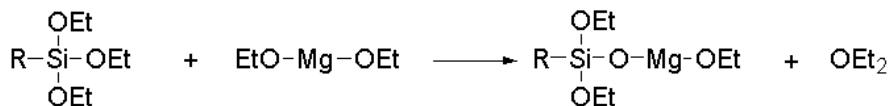
Fig. 4 High resolution XPS spectra in the P (2p) region of MgOEt + SiP system calcined at 260 and 450 °C and of MgAc + SiP system calcined at 260 and 450 °C

involved in the reaction between SiP and magnesium ethoxide or magnesium acetate. The Si (2p) and Mg (2s) regions are presented in Figure S3 of the Supplementary Information. For the Si (2p) region, a single signal centered at 102.7 eV was observed for all samples and it was attributed to silicon atom linked to an oxygen atom [32]. There is no variation of binding energy in the Mg (2s) region. A single peak centered at 89.4 eV assigned to a magnesium atom linked to an oxygen atom [33] was observed.

To conclude, XPS analyses on thermally treated systems clearly confirmed that the reaction between silicon and magnesium inorganic precursors formed chemical bonds of interest, such as Si-O-Mg. The phosphonate group of SiP is not involved in the reaction in our experimental conditions. In agreement with the TGA-GC-MS analyses, by-products produced during the reaction were solely due to the reaction between the ethoxysilane groups of SiP and ethoxy and acetoxy groups of magnesium ethoxide or magnesium acetate, respectively.

Elucidated reaction schemes are presented in **Fig. 5**. According to the TGA-GC-MS and XPS analyses, it was assumed that the reaction between SiP and magnesium ethoxide followed a non-hydrolytic sol-gel route through a thermal activation. Indeed, the reaction occurs between the ethoxy groups of the alkoxy silane and the ethoxy groups of the magnesium precursor. The elimination of diethyl ether as a by-product of reaction supports this claim. Concerning the reaction between SiP and magnesium acetate, in a first stage, water of the tetrahydrate Mg precursor hydrolyzes the ethoxy groups of the alkoxy silane leading to the release of ethanol. Then, acetoxy groups of MgAc reacts with the SiP through a classical inorganic sol-gel route to finally released ethyl acetate as a by-product.

a)



b)

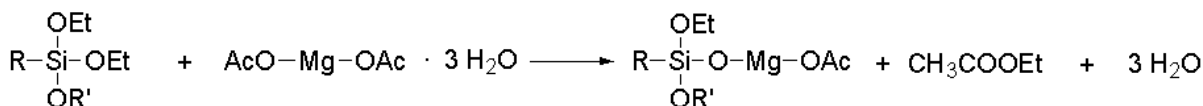
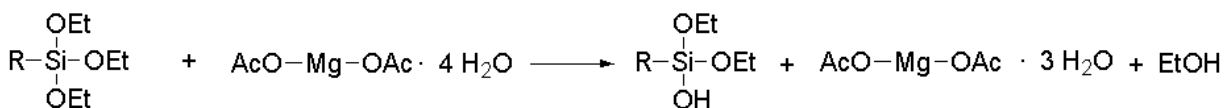


Fig. 5 Elucidated reaction schematics between SiP and MgEt (a) and SiP and MgAc (b) with R = CH₂CH₂PO(OEt)₂ and R' = OH or OEt

The conversion through the evaluation of by-products concentration by TGA-GC-MS was completed by the analysis of the condensation rate obtained through the XPS analysis. The various chemical forms of magnesium were obtained after the previous detailed deconvolution of the Mg (1s) signal (**Fig 3**). Their relative abundance was expressed as the ratio of the area of each deconvoluted peak to the total area of the

original signal. They are reported in Table 3. These results showed that the synthesized oxides are mainly constituted of Mg-O-Si chemical bonds and marginally composed of Mg-O-Mg bonds. The high dispersion of values did not enable to confirm of an increase of the Si-O-Mg bonds percent with increasing temperature but confirmed an abundance of formation of interest's bonds. In the literature, the same trend was observed [16]. Actually, silica-magnesia mixed oxides prepared from MgCl₂ and TEOS present Si-O-Mg signal in XPS but also Mg-O-Mg bonds. The reaction was performed in ethanol with ammonium hydroxide at ambient temperature for 24 hours. Authors evidenced thus the formation of magnesium silicates moieties and pure magnesia moieties. In our case, obtained results confirm again that the sol-gel process has been mostly employed during the reaction.

Table 3 Chemical forms of Mg (1s) expressed as a percentage of relative form to the total area of the peak for both systems treated respectively at 260 and 450 °C (two analyses of each) (after respectively almost 25 and 40 min of reaction according to the heating up during the TGA)

	Analysis number	Si-O-Mg (%)	Mg-O-Mg (%)
MgOEt + SiP treated at 260 °C	1	76	24
	2	79	21
MgOEt + SiP treated at 450 °C	1	92	9
	2	77	23
MgAc + SiP treated at 260 °C	1	91	9
	2	91	9
MgAc + SiP treated at 450 °C	1	68	32
	2	58	42

2) Kinetics of the reaction followed by DMA and determination of gel point

A complementary interesting approach to follow the reaction expected in this study was to scrutinize the evolution of the viscoelastic behavior and the determination of the gel point.

In details, to get a further view of the type of structure created during the sol-gel reaction between the precursors, the change of viscoelastic behavior of the material during the reaction was followed. The analysis was started after 15 min of reaction at 120, 150 and 170 °C. Before this time, the mixture was not enough viscous to record a measurable signal in the rheometer.

Firstly, frequency sweep, starting at the highest frequency of 100 rad/s, was performed to follow the evolution of the storage (G') and loss (G'') modulus. The duration of such an experiment was approximately 70 and 90 min for MgAc + SiP and MgOEt + SiP reactions, respectively. At the end of this step, a second frequency sweep was performed in the same conditions, in order to evidence any irreversible structural change. Especially, information about the structure, and occurrence of a physical or chemical gelation might

be collected. Because of the duration of the experiments, frequency sweeps also acted indirectly as time sweep experiments since the sol-gel reaction was constantly evolving during the experiment. For this reason, a time axis was presented on the top of the graph presenting the frequency sweeps.

Fig. 6 shows the frequency sweeps during the reaction between SiP and magnesium ethoxide at the various temperatures.

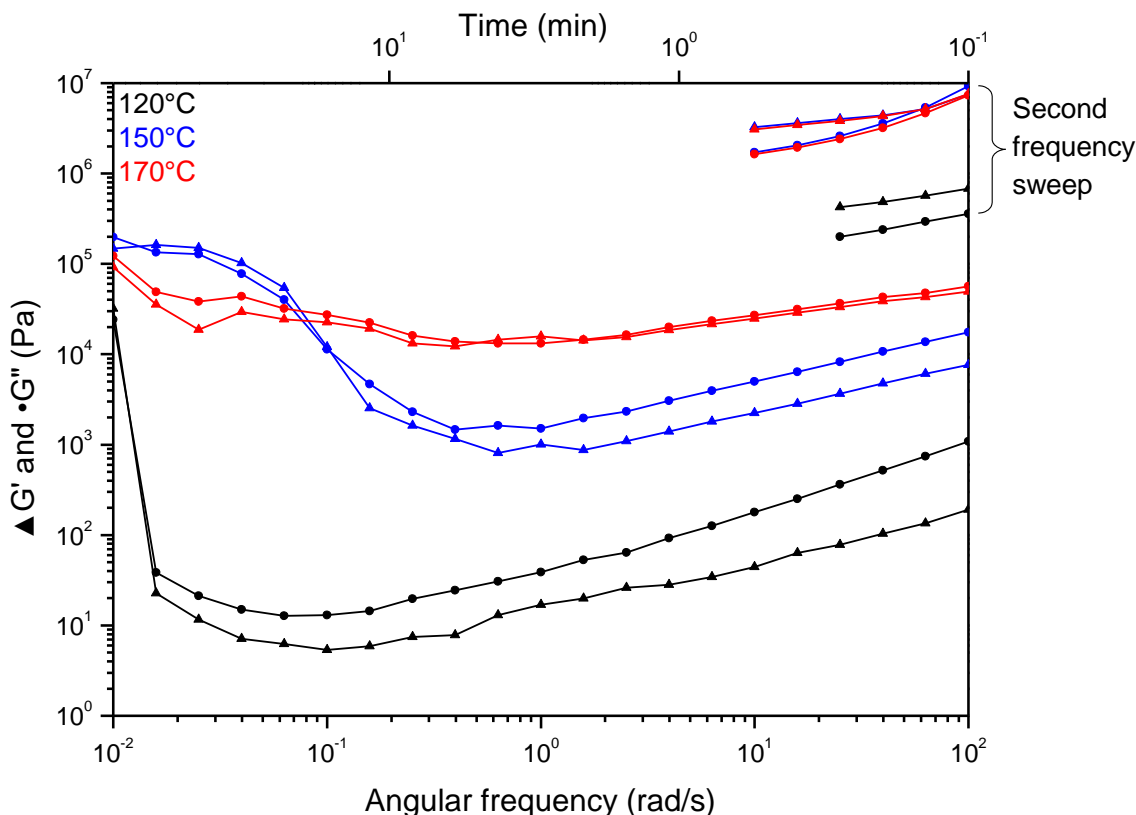


Fig. 6 Frequency sweep under air of MgOEt + SiP after 15min of reaction at 120, 150 and 170 °C

Generally, at constant frequency (and reaction time) when the temperature increased, both storage and loss dynamic moduli, G' and G'' , also increased. For example, at 100 rad/s, G' increased from 200 Pa at 120 °C up to 7600 Pa at 150 °C and up to 49500 Pa at 170 °C. Without structural change, the modulus at constant frequency should have decreased with temperature, therefore this indicated a reaction. Moreover, the raise of moduli indicated a higher degree of reaction advancement at higher temperature. At high frequencies, the loss modulus G'' was larger than the storage modulus G' pointing out that the system was in a liquid state and mostly viscous. When the frequency decreased, both moduli decreased and leveled off to a plateau at low frequency. After this plateau, G' and G'' strongly increased showing that the system underwent a thickening and became more viscous and elastic. At this point, G' overpassed G'' revealing a gel point at which the system passed from a viscous behavior to an elastic one. At the highest temperature, 170 °C, these features were less visible, G' and G'' were almost equal independently of the frequency even at the earliest times because the reaction was already in a sufficiently advanced stage.

At the beginning of the second frequency sweep, 90 min after the starting of the first experiment, for all temperatures, moduli were higher than ones obtained at the end of the first sweep. This evidenced that the structure had been chemically crosslinked and that the modifications undergone by the system were irreversible indicating chemical gelation.

Systems with magnesium acetate presented similar behavior (**Fig.7**).

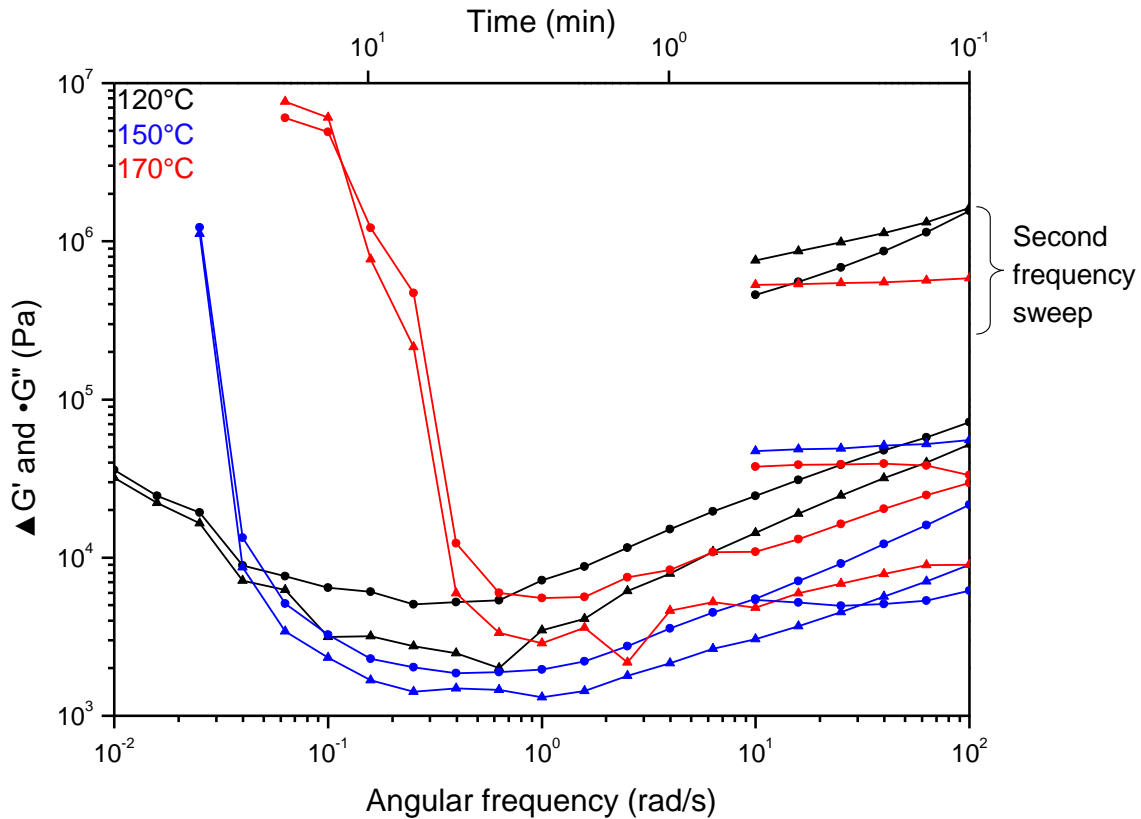


Fig. 7 Frequency sweep under air of MgAc + SiP after 15min of reaction at 120, 150 and 170 °C

Indeed, at high frequencies, the loss modulus G'' was higher than the storage modulus G' for all temperatures indicating that systems behaved mainly as a viscous liquid. When the angular frequency decreased, but simultaneously the reaction time increased, moduli decreased accordingly and leveled off to a plateau then rapidly increased for measurements performed at 150 and 170 °C. G' became higher than G'' meaning that systems underwent thickening and became elastic. At 120 °C, this increase was not as sharp as much. Moreover, from the time axis, it was seen that this thickening occurred earlier when the temperature was high. Actually, at 150 °C the increase of moduli started at around 10 minutes against 4 minutes at 170 °C. This shift to lower times when temperature increased indicated that the sol-gel reaction was more advanced at high temperature. At the beginning of the second frequency sweep, all moduli were greater or equal to the value obtained at the end of the first sweep. Also, G' was still higher than G'' indicating that the systems kept their elastic behavior during this second run. Thus, the modifications were irreversible and chemical gelation had occurred.

The analysis of the kinetics of the reaction by rheological means demonstrated the formation of chemical gels but were also used to determine the gel point by performing viscoelastic measurement in oscillatory shear during time sweeps.

The rheological behavior of a system that underwent physical or chemical gelation can be described as in [33-35]. At the beginning of the reaction, for polymeric chemical gels, only monomers or un-crosslinked polymer chains were present in the reaction media. The system behaved as a viscoelastic liquid and the variation of the dynamic moduli can be described as:

$$G' \sim \omega^2 \quad \text{Eq. 5}$$

$$G'' \sim \omega^1 \quad \text{Eq. 6}$$

where ω is the angular frequency.

Beyond the gel point, the system presents a dominantly elastic solid behavior with a constant elastic modulus G' and a power law dependence towards frequency for the viscous modulus G'' :

$$G' \sim \omega^0 \quad \text{Eq. 7}$$

$$G'' \sim \omega^1 \quad \text{Eq. 8}$$

Between these two behaviors, at the gel point, both G' and G'' have the same power law dependence with the frequency:

$$G' \sim G'' \sim \omega^\Delta \quad \text{Eq. 9}$$

with $\Delta = \frac{2\delta}{\pi}$ ranging from 0 (elastic gel) and 1 (viscous gel), being called the gel exponent.

The loss angle is:

$$\delta = \tan^{-1} \left(\frac{G''}{G'} \right) \quad \text{Eq. 10}$$

Because at the gel point G' and G'' have the same dependence towards frequency, $\tan(\delta)$ should be frequency independent at the gel point. In other words, a plot of $\tan(\delta)$ measured at various frequencies as a function of time, should lead to curves intersecting at a unique point defining the gel time.

The power law behavior of the G' and G'' moduli reflect the fact that there is no particular time scale or size scale characteristic of the material at gel time. The growth of the clusters which participate to the formation of the gel can be described in terms of fractal geometry. The molecular mass M and radius R of a fractal cluster are related by $M \sim R^{d_f}$ where d_f is the fractal dimension of the cluster. Muthukumar [37] determined a relationship between the gel exponent and the fractal dimension d_f . In the case where the excluded volume is screened, the equation for a three-dimensional space is:

$$d_f = \frac{5}{2} \left[\frac{2\Delta - 3}{\Delta - 3} \right] \quad \text{Eq. 11}$$

The fractal dimension at the gel point was claimed to be $d_f = 2$ in the case of poly(dimethylsiloxane) (PDMS) clusters [34]. This value of d_f was used in this work as a criterion of gelation to compare with the

experimental results. Then, if the fractal dimension is superior or equal to 2, it is assumed that they reached their gel point.

Fig. 8 represents the evolution of $\tan(\delta)$ versus time at 120, 150 and 170 °C at different frequencies during the reaction of the MgOEt + SiP mixture. In general terms, for all temperatures, $\tan(\delta)$ decreased with time. More specifically, after a certain time, a more or less slight increase of $\tan(\delta)$ was observed. It was attributed to an increase of viscosity related to an increase of the molar mass that overpassed the change of elasticity. Intersection of curves in this region cannot be attributed to a gel point. After this slight increase, $\tan(\delta)$ decreased. At 120 °C, no clear intersection point was observed. Also, in this case, at the end of the time sweep, $\tan(\delta)$ was much higher than 1, and therefore d_f was lower than 2. Thus, MgOEt + SiP system did not reach any gel point within the studied time range. At 150 °C, $\tan(\delta)$ was about 1.5 at the end of sweep, and the fractal dimension was 1.8, near to the gel point but the curves did not intersect clearly at a single point. At 170 °C, within experimental errors, an intersection point of $\tan(\delta)$ was observed at 2150 seconds. At this point, $\tan(\delta) = 0.85$ and so $d_f = 2.06$. Therefore, at 2150 seconds, i.e. almost 36 minutes, the reaction between magnesium ethoxide and SiP underwent its sol-gel transition. Concerning storage and loss moduli, in general terms, the higher the temperature was, the higher G' and G'' values were, indicating the influence

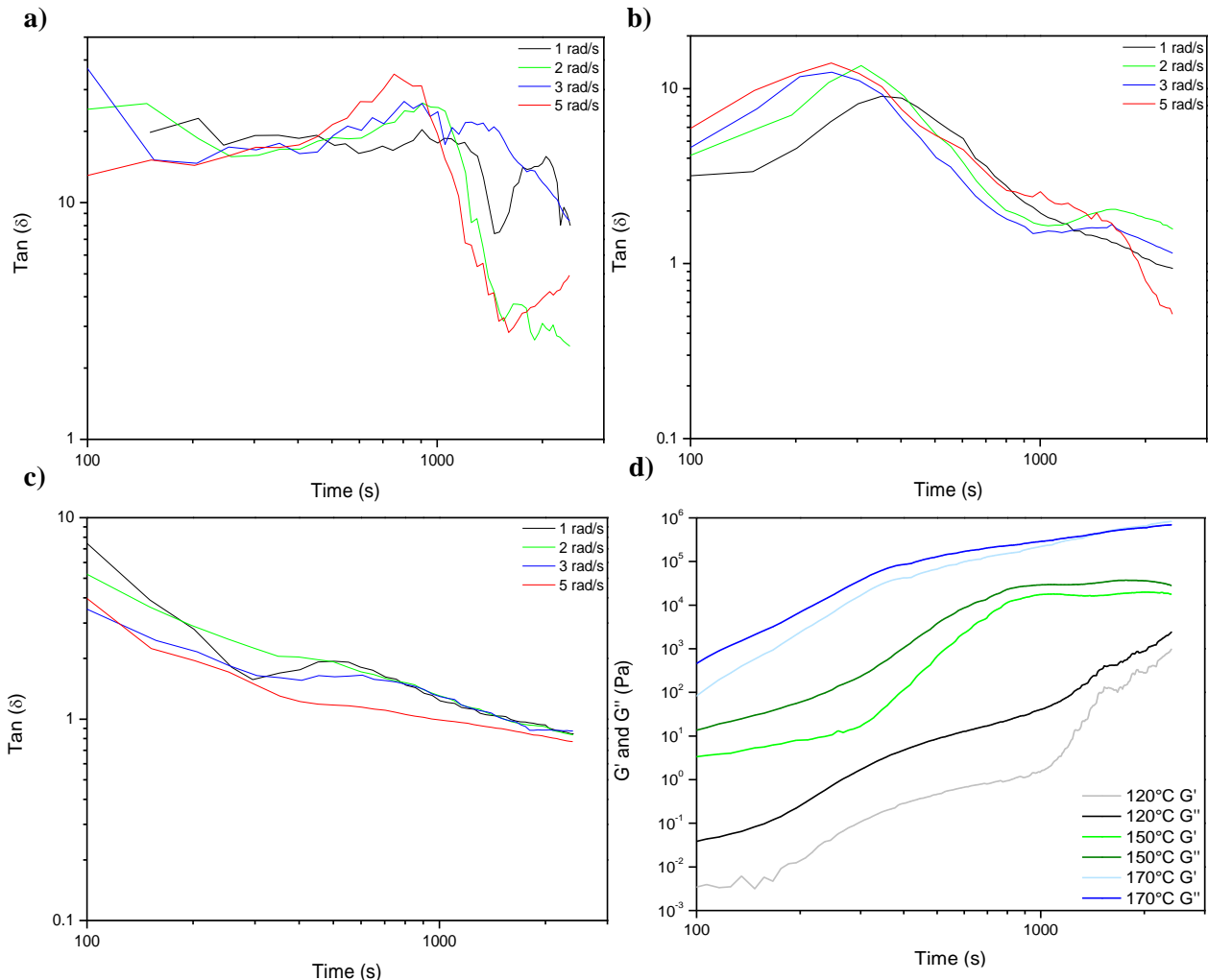


Fig. 8 Evolution of $\tan(\delta)$ at 120 °C (a) 150 °C (b) and 170 °C (c) during time sweeps at 1, 2, 3 and 5 rad/s and evolution of the corresponding elastic and viscous moduli at 2 rad/s (d) for MgOEt + SiP system

of temperature on the extent of reaction. At 120 °C, moduli remained constants at the beginning. After about 200 seconds, they sharply increased.

This phenomenon was also observed by Khan *et al.* [38] and Hodgson *et al.* [39] for fluorine-doped silicate system and tetraethoxysilane and has been ascribed to the formation of a chemically gelling system. Moreover, during all the time sweep, G'' remained higher than G' which indicated the mainly viscous behavior of the system. At 150 °C, several steps were observed on the moduli evolution. At short times, moduli increased only slightly. Then, after 300 seconds, they rapidly grew and reached a plateau. During the whole sweep, the behavior of the sample was mainly viscous. At 170 °C, G' and G'' increased in two steps: first, a rapid growth was observed and then at about 300 seconds, the increase was less important. At the end of the experiment, G' crosses G'' indicating the vicinity of the sol-gel transition.

For the reaction with magnesium acetate, the unreacted liquid mixture had a very low viscosity and could not be kept properly between the rheometer plates. During the heating of the chamber of the rheometer, important quantity of volatile products escaped (mainly water and the first part of ethanol as established by TGA-GC-MS, Fig. 2) from the plates and led to formation of bubbles and voids at the surface of the plates. To prevent this problem, the samples were pre-reacted during 7 minutes in a flask heated by an oil bath at 120, 150 and 170 °C. Referring to the Figure S5 of the Supplementary Information, after this reaction time, a major part of volatile was released and then samples were properly kept between rheometer plates.

Fig 9 shows the evolution of $\tan(\delta)$ as a function of time of the MgAc + SiP systems after 7 minutes of pre-reaction. The behavior was similar to that with magnesium ethoxide. Indeed, at 120 °C, the gel point was not reached in the studied time range since curves did not cross at a precise point. At 150 °C, a crossing point was observed at around 1000 seconds, though this time could not be the gel time because $\tan(\delta)$ increased after this point. As stated previously, this increase of $\tan(\delta)$ can be attributed to a growth of molar mass. At the end of the measurement, there was no intersection of curves at a single time. Conversely, at 170 °C, the gel point was clearly seen at 600 seconds.

At this time, $\tan(\delta) = 0.31$ and $d_f = 2.33$ and thus, the system reached the sol-gel transition. As the sample was pre-reacted for 7 minutes, the true gel point of MgAc + SiP at 170 °C was 1020 seconds, i.e., 17 minutes.

Concerning storage and loss moduli, they constantly increased at 120 °C indicating the system thickening. At 150 °C, the increases of moduli followed two steps: at first, a slight increase was observed and after almost 900 s, moduli grewed sharply. At 170 °C, after an induction time of almost 200 s, G' and G'' rapidly increased and then reached a plateau where G' was higher than G'' indicating an elastic solid behavior.

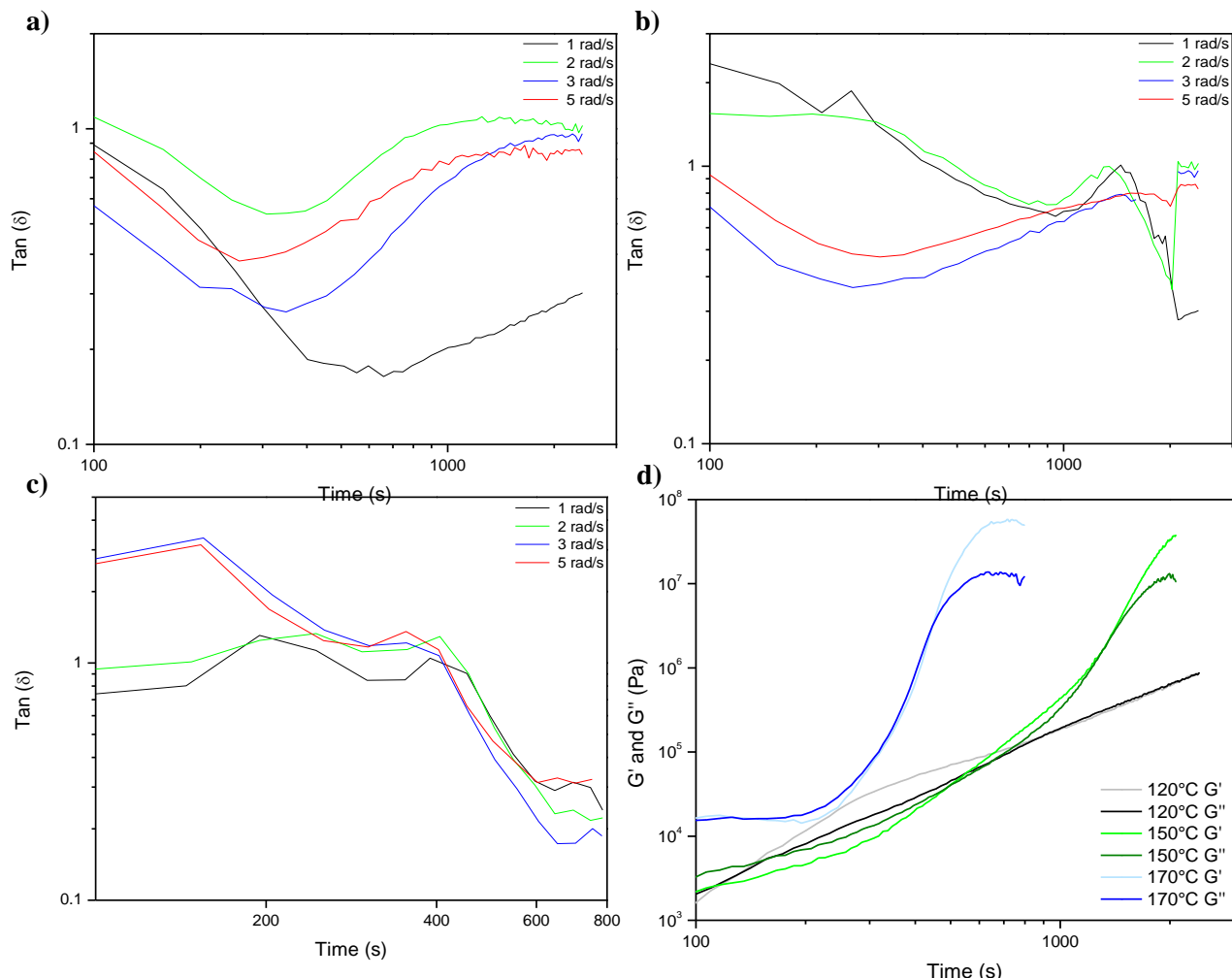


Fig. 9 Evolution of $\tan(\delta)$ at 120 °C (a) 150 °C (b) and 170 °C (c) during time sweeps and evolution of the corresponding elastic and viscous moduli at 2 rad/s (d) for MgAc + SiP system pre-reacted for 7 min

IV. Conclusion

In the present work, we proposed to synthesize new chemical systems containing Si-O-Mg bonds by using sol-gel chemistry. For that, two different magnesium oxide inorganic precursors were used: magnesium ethoxide and magnesium acetate tetrahydrate. Diethylphosphatoethyltriethoxysilane was used as a silica inorganic precursor. By-products of interest were detected and confirmed the reaction between precursors. Indeed, appearance of diethyl ether and ethyl acetate confirmed the reaction between functional groups of organic precursors. Isothermal measurements showed high conversion rates, i.e., 60.9 and 66.7 % at 170 °C for the system with magnesium ethoxide and magnesium acetate respectively.

To confirm the formation of Si-O-Mg bonds, XPS analyses were performed and indicate that the reaction occurred between the ethoxysilane groups of SiP and the ethoxy or acetoxy groups of magnesium ethoxide and magnesium acetate, respectively. The ethyl phosphonate group of SiP remained unreacted and did not take part in the reaction. A small amount of Mg-O-Mg bonds were created by the condensation of the

magnesium oxide inorganic precursor itself, independently of the reaction with SiP. The residue rate obtained by TGA also corroborated the formation of an inorganic network.

Furthermore, viscoelastic measurements performed during the reaction showed that both systems underwent thickening during frequency sweeps. This thickening was associated to the chemical gelation. The gel point was determined by following $\tan(\delta)$ as a function of time. For both systems, sol-gel transition is observed only at 170 °C, namely at 2150 s and 1020 s for magnesium ethoxide + SiP and magnesium acetate + SiP reactions. All these data are very promising results to further elaborate polymer based composites by the *in situ* creation of filler by sol-gel chemistry at quite low synthesis temperature. In that frame, soft inorganic network will be expected as we will demonstrate in a next coming study.

References

1. Coradin T, Boissiere M, Livage J (2009) Sol-gel Chemistry in Medicinal Science. *Curr Med Chem*. <https://doi.org/10.2174/092986706789803044>
2. Nair PAK, Vasconcelos WL, Paine K, Calabria-Holley J (2021) A review on applications of sol-gel science in cement. *Constr Build Mater*. <https://doi.org/https://doi.org/10.1016/j.conbuildmat.2021.123065>
3. Rull N, Sánchez-Ferrer A, Frontini PM (2020) Deformation behavior of crosslinked polyurea elastomers obtained via sol-gel chemistry: Experimental determination and constitutive modelling. *Express Polym Lett*. <https://doi.org/10.3144/expresspolymlett.2020.54>
4. Giordano C, Antonietti M (2011) Synthesis of crystalline metal nitride and metal carbide nanostructures by sol-gel chemistry. *Nano Today* 6:366–380
5. Brinker CJ, Scherer GW (1990) *Sol-Gel Science: The Physics and Chemistry of Sol-Gel Processing*, Academic Press
6. Esposito S (2019) "Traditional" sol-gel chemistry as a powerful tool for the preparation of supported metal and metal oxide catalysts. *Mater*. <https://doi.org/https://doi.org/10.3390/ma12040668>
7. Danks AE, Hall SR, Schnepf Z (2016) The evolution of 'sol-gel' chemistry as a technique for materials synthesis. *Mater Horizons*. <https://doi.org/10.1039/C5MH00260E>
8. Hench LL, West JK (1990) The Sol-Gel Process. *Chem Rev*. <https://doi.org/10.1021/CR00099A003>
9. Nedelec JM (2007) Sol-gel processing of nanostructured inorganic scintillating materials. *J Nanomater*. <https://doi.org/10.1155/2007/36392>
10. Styskalik A, Skoda D, Barnes CE, Pinkas J (2017) The Power of Non-Hydrolytic Sol-Gel Chemistry: A Review. *Catalysts*. <https://doi.org/10.3390/CATAL7060168>
11. Debecker DP, Mutin PH (2012) Non-hydrolytic sol-gel routes to heterogeneous catalysts. *Chem Soc Rev*. <https://doi.org/10.1039/c2cs15330k>
12. Mutin PH, Vioux A (2009) Nonhydrolytic Processing of Oxide-Based Materials: Simple Routes to Control Homogeneity, Morphology, and Nanostructure. *Chem Mater*.

<https://doi.org/10.1021/CM802348C>

13. Gross S, Müller K (2011) Sol-gel derived silica-based organic-inorganic hybrid materials as composite precursors for the synthesis of highly homogeneous nanostructured mixed oxides: An overview. *J Sol-Gel Sci Technol.* <https://doi.org/10.1007/S10971-011-2565-X>
14. Fujiwara M, Wessel H, Park HS, Roesky HW (2002) A Sol-Gel Method Using Tetraethoxysilane and Acetic Anhydride: Immobilization of Cubic μ -Oxo Si-Ti Complex in a Silica Matrix. *Chem Mater.* <https://doi.org/10.1021/CM020424N>
15. Lopez T, Manriquez ME, Gomez R, et al (2000) Sol-gel copper-magnesia-silica mixed oxides. *Mater Lett* 46:21–29
16. Brambilla R, Radtke C, dos Santos JHZ, Miranda MSL (2010) Silica-magnesia mixed oxides prepared by a modified Stöber route: Structural and textural aspects. *Powder Technol.* <https://doi.org/10.1016/j.powtec.2009.11.029>
17. Niederberger M, Garnweitner G (2006) Organic reaction pathways in the nonaqueous synthesis of metal oxide nanoparticles. *Chem – A Eur J.* <https://doi.org/10.1002/CHEM.200600313>
18. Lopez T, Navarrete J, Gomez R, et al (1995) Preparation of sol-gel sulfated ZrO₂-SiO₂ and characterization of its surface acidity. *Appl Catal A Gen.* [https://doi.org/10.1016/0926-860X\(95\)00022-4](https://doi.org/10.1016/0926-860X(95)00022-4)
19. Voigt A, Murugavel R, Chandrasekhar V, et al (1996) Facile and rational route for high-yield synthesis of titanasiloxanes from aminosilanetriols. *Organometallic.* <https://doi.org/10.1021/OM950816M>
20. Kim WS, Yoon KB, Bae BS (2005) Nanopatterning of photonic crystals with a photocurable silica-titania organic-inorganic hybrid material by a UV-based nanoimprint technique. *J Mater Chem.* <https://doi.org/10.1039/B509622G>
21. Nampi PP, Moothetty P, Berry FJ, et al (2010) Aluminosilicates with varying alumina-silica ratios: Synthesis via a hybrid sol-gel route and structural characterisation. *Dalt Trans.* <https://doi.org/10.1039/C001219J>
22. Bounor-Legaré V, Cassagnau P (2014) In situ synthesis of organic-inorganic hybrids or nanocomposites from sol-gel chemistry in molten polymers. *Prog Polym Sci.* <https://doi.org/10.1016/j.progpolymsci.2014.04.003>
23. Ciesielczyk F, Przybysz M, Zdarta J, et al (2014) The sol-gel approach as a method of synthesis of xMgO·ySiO₂ powder with defined physicochemical properties including crystalline structure. *J Sol-Gel Sci Technol.* <https://doi.org/10.1007/s10971-014-3398-1>
24. Huang X, Men Y, Wang J, et al (2017) Highly active and selective binary MgO-SiO₂ catalysts for the production of 1,3-butadiene from ethanol. *Catal Sci Technol.* <https://doi.org/10.1039/c6cy02091g>
25. Garnier A, Da Cruz-Boisson F, Rigolet S, et al (2016) Hydrolysis-condensation reactions of diethylphosphato-ethyltriethoxysilane involved in organic-inorganic talc-like hybrid synthesis: liquid and solid-state NMR investigations. *R Soc Chem.* <https://doi.org/10.1039/C6RA12719C>
26. Jung HS, Lee JK, Kim JY, Hong KS (2003) Crystallization behaviors of nanosized MgO particles from magnesium alkoxides. *J Colloid Interface Sci.* [https://doi.org/10.1016/S0021-9797\(03\)00034-](https://doi.org/10.1016/S0021-9797(03)00034-)

27. Isa K, Nogawa M (1984) Thermal decomposition of magnesium acetate tetrahydrate under self-generated atmosphere. *Thermochim Acta*. [https://doi.org/10.1016/0040-6031\(84\)85020-0](https://doi.org/10.1016/0040-6031(84)85020-0)
28. Hewitt F, Rhebat DE, Witkowski A, Hull TR (2016) An experimental and numerical model for the release of acetone from decomposing EVA containing aluminium, magnesium or calcium hydroxide fire retardants. *Polym Degrad Stab*. <https://doi.org/10.1016/j.polymdegradstab.2016.01.007>
29. Moulder JF, Stickle WF, Sobol PE', Bomben KD (1992) *Handbook of X-ray Photoelectron Spectroscopy A Reference Book of Standard Spectra for Identification and Interpretation of XPS Data*, Chastain
30. Khairallah F, Glisenti A (2007) Synthesis, characterization and reactivity study of nanoscale magnesium oxide. *J Mol Catal A Chem*. <https://doi.org/10.1016/j.molcata.2007.04.039>
31. Khramov AN, Balbyshev VN, Kasten LS, Mantz RA (2006) Sol-gel coatings with phosphonate functionalities for surface modification of magnesium alloys. *Thin Solid Films*. <https://doi.org/10.1016/j.tsf.2006.02.023>
32. Klopogge JT, Wood BJ (2020) *Handbook of Mineral Spectroscopy - Volume 1: X-ray Photoelectron Spectra*. Elsevier
33. Le Febvrier A, Jensen J, Eklund P (2017) Wet-cleaning of MgO(001): Modification of surface chemistry and effects on thin film growth investigated by x-ray photoelectron spectroscopy and time-of-flight secondary ion mass spectroscopy. *J Vac Sci Technol A*. <https://doi.org/10.1116/1.4975595>
34. Muthukumar M, Winter HH (1986) Fractal Dimension of a Cross-Linking Polymer at the Gel Point. *Macromolecules*. <https://doi.org/10.1021/ma00158a064>
35. In M, Prud'homme RK (1993) Fourier transform mechanical spectroscopy of the sol-gel transition in zirconium alkoxide ceramic gels. *Rheol Acta*. <https://doi.org/10.1007/BF00369072>
36. Payet L, Ponton A, Agnely F, et al (2002) Caractérisation rhéologique de la gélification d'alginate et de chitosane : effet de la température. *Rhéologie* 2:46–51
37. Muthukumar M (1989) Screening Effect on Viscoelasticity near the Gel Point. *Macromolecules*. <https://doi.org/10.1021/ma00202a050>
38. Khan SA, Prud'homme RK, Rabinovich EM, Sammon MJ (1989) Rheology of the gelation of fluorine-doped silica sols. *J Non Cryst Solids*. [https://doi.org/10.1016/0022-3093\(89\)90251-2](https://doi.org/10.1016/0022-3093(89)90251-2)
39. Hodgson DF, Amis EJ (1991) Dynamic viscoelasticity during sol-gel reactions. *J Non Cryst Solids*. [https://doi.org/10.1016/0022-3093\(91\)90702-8](https://doi.org/10.1016/0022-3093(91)90702-8)

Statements & Declarations

Funding

The authors are grateful to Nexans for the financial support in this project.

Competing Interests

The authors have no relevant financial or non-financial interests to disclose.

Author Contributions

All authors contributed to the study conception and design. Material preparation, data collection and analysis were performed by Busra Findik. The first draft of the manuscript was written by Busra Findik and all authors commented on previous versions of the manuscript. All authors read and approved the final manuscript.

Solvent Free Sol-Gel Based Synthesis of Soft Magnesium Silicate

Supplementary Information

Busra Findik^{1,3}, Valentin Cinquin¹, Franck Gyppaz³, Christian Carrot², Véronique Bounor-Legaré^{1*}

(1) Univ Lyon, CNRS, UMR 5223, Ingénierie des Matériaux Polymères, Université Claude Bernard Lyon 1, INSA Lyon, Université Jean Monnet, F-69622 VILLEURBANNE Cédex, France

(2) Univ Lyon, CNRS, UMR 5223, Ingénierie des Matériaux Polymères, Université Claude Bernard Lyon 1, INSA Lyon, Université Jean Monnet, F-42023 SAINT-ETIENNE Cédex 2, France

(3) Nexans Research Center, Nexans France, F-69007 LYON, France

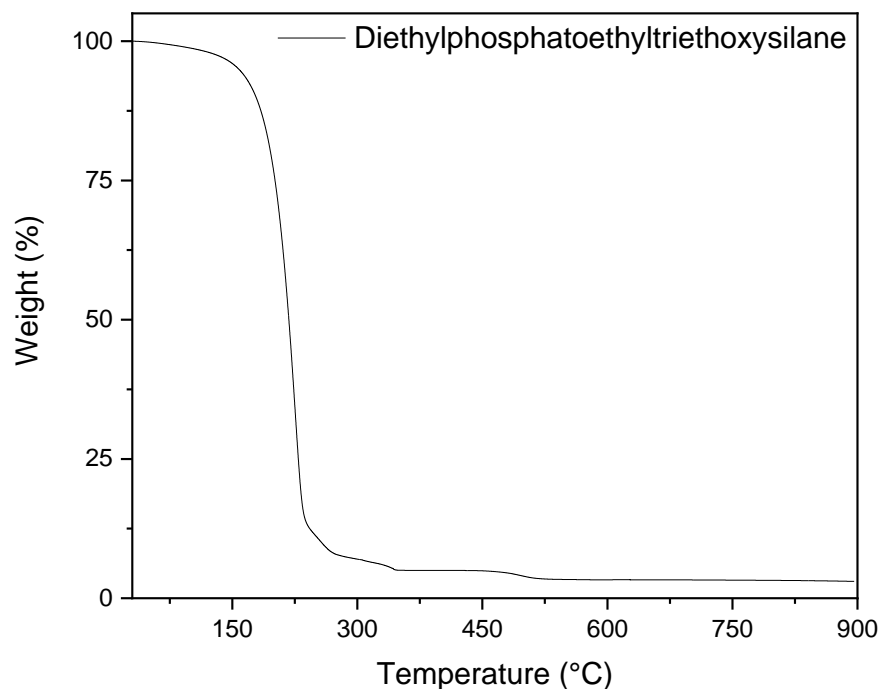


Figure S1 – Thermogram of diethylphosphatoethyltriethoxysilane under He at 10 °C/min

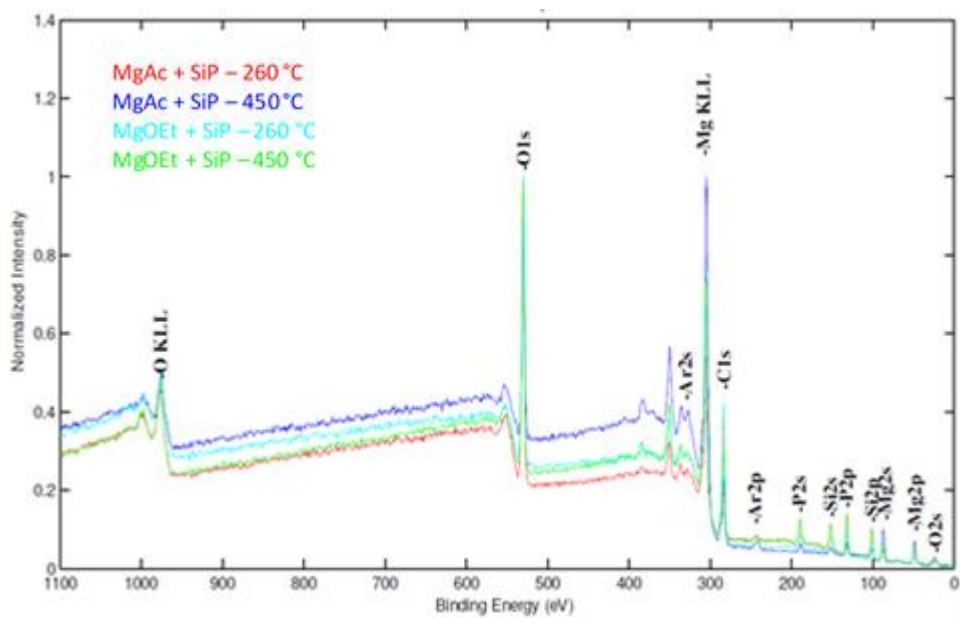


Figure S2 - Wide scan spectrum of MgOEt + SiP and MgAc + SiP systems heat treated over He flow at 260 and 450 °C

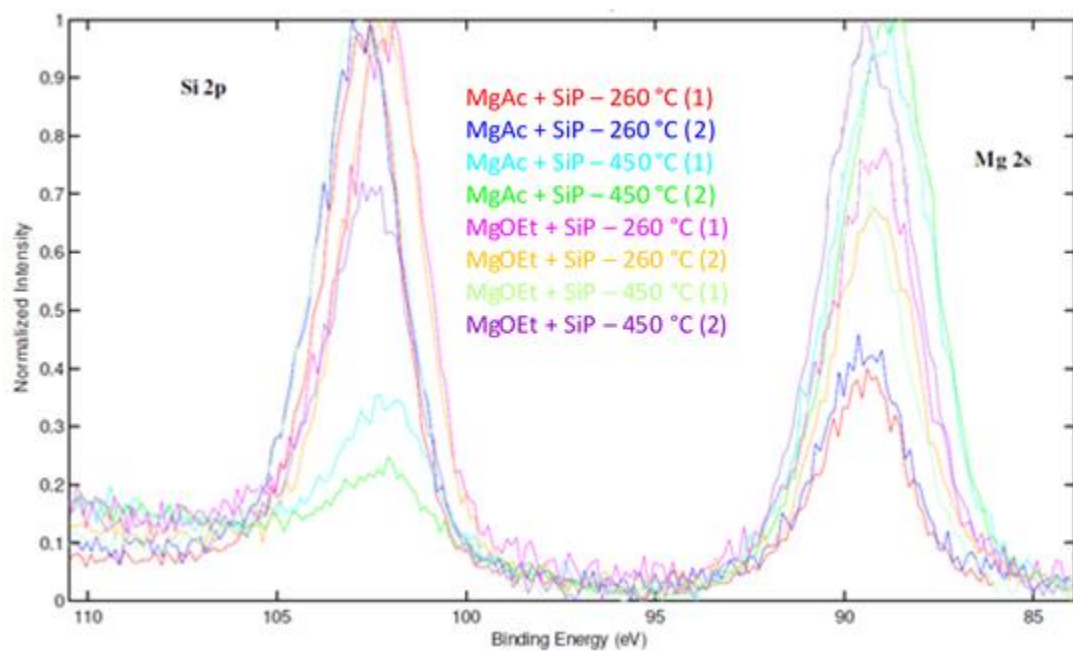


Figure S3 - High resolution XPS spectra in the Si (2p) and Mg (2s) regions of heat treated over He flow MgOEt + SiP system at 260 and 450°C and of MgAc + SiP system at 260 and 450°C

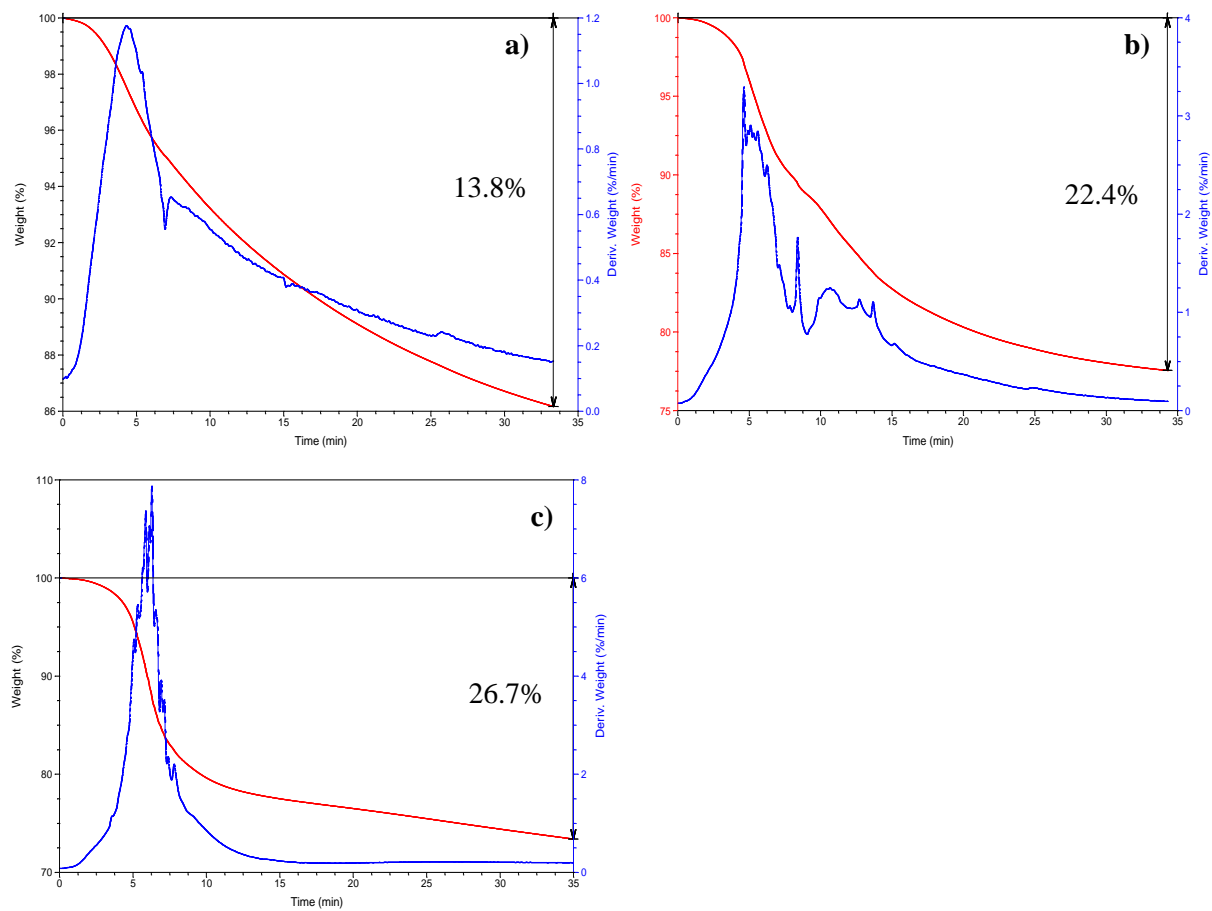


Figure S4 - Isothermal thermograms of MgOEt + SiP system at 120 °C (a) 150 °C (b) and 170 °C (c) under He

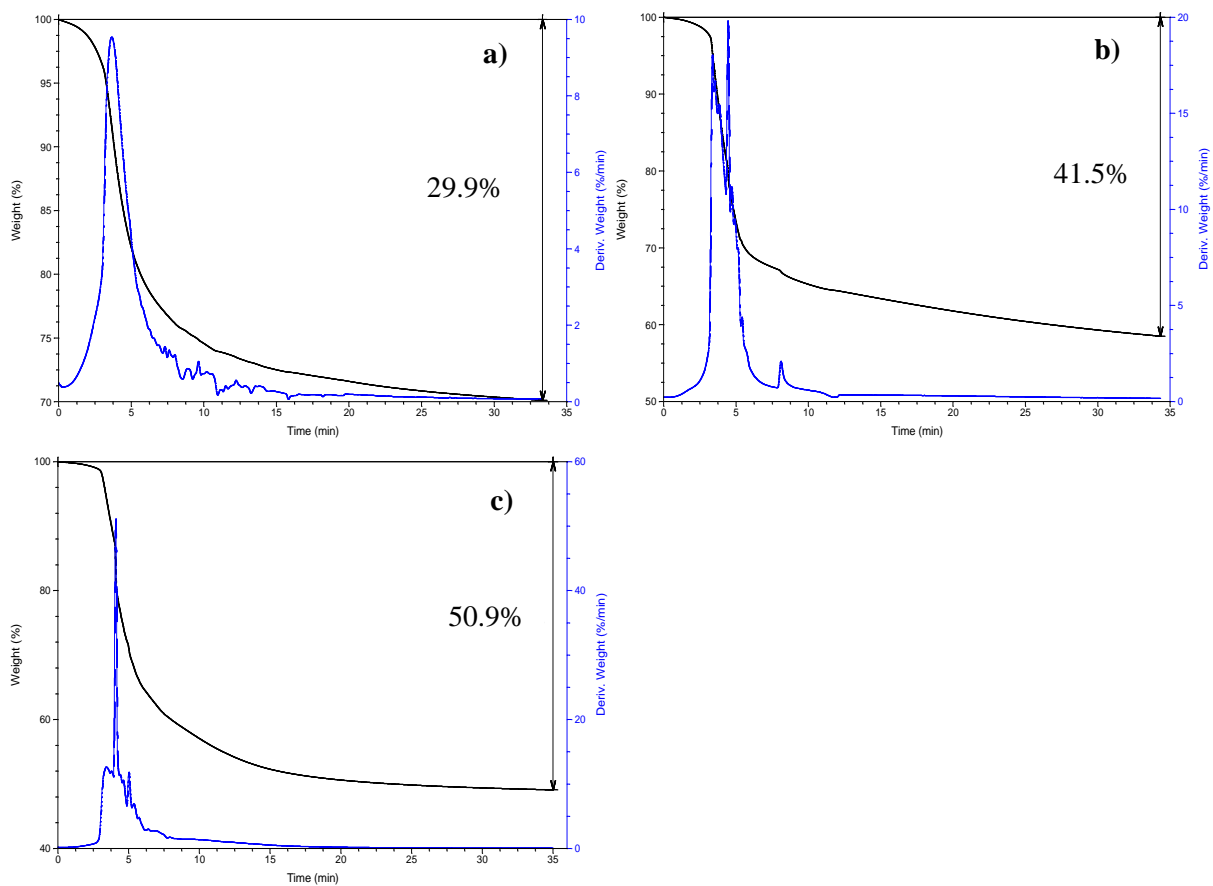


Figure S5 - Isothermal thermograms of MgAc + SiP system at 120 °C (a) 150 °C (b) and 170 °C (c) under He